WATER RESOURCES RESEARCH, VOL. 25, NO. 9, PAGES 1937–1946, SEPTEMBER 1989

A Composite Analytical Model for Analysis of Pumping Tests Affected by Well Bore Storage and Finite Thickness Skin

KENT S. NOVAKOWSKI

National Water Research Institute, Burlington, Ontario, Canada

A composite analytical model is developed for analyzing the results of pumping tests where the influence of well bore storage and a skin region of finite thickness are present at the pumping well. The solution of the boundary value problem for dimensionless drawdown in the pumping well, skin region, and formation is derived using the Laplace transform method. The solution is verified by comparison to solutions of pumping test problems with well bore storage only, with a composite formation only, and with well bore storage and infinitesimally thin skin. Type curves obtained by numerically inverting the solution for drawdown in the formation are used to illustrate the influence of well bore storage, the effect of skin region characteristics, and the effect of radial distance. These show that the influence of a finite thickness skin of reduced permeability is clearly identifiable over a fairly broad range of radial distance from the pumping well when well bore storage effects are minimized. Conversely, the effects of finite skin of enhanced permeability are more easily identified where the influence of well bore storage is greater. In both cases the type curves are uniquely defined provided that the skin region is of nonzero thickness. Type curves obtained for the solution for drawdown in the skin region are used to illustrate the effect of outer or far-field boundary conditions. These type curves show that early time data not influenced by well bore storage effects are required to detect the presence of outer boundaries of reduced permeability. Drawdown data at late time, although less influenced by well bore storage effects, are subject to nonuniqueness with regard to the characteristics of the skin and formation regions. Outer boundaries of enhanced permeability are identified only at early time and are almost entirely masked by well bore storage at later time.

INTRODUCTION

The most commonly used method to measure the transmissivity and storativity of a geological formation between two or more wells is the pumping test. With this method, the withdrawal of water from the pumping well is presumed to influence the hydraulic head in the formation in a direct instantaneous relation; i.e., the pumping well is of infinitesimal radius and acts as a line source. Assuming the formation is homogeneous, isotropic, confined, of infinite extent, and single porosity, only one type curve (the Theis curve) is required for analysis of pumping test results using this method. Clearly, because pumping wells are always of nonzero diameter, this assumption may lead to some error in test analysis. However, for pumping tests conducted in high-storativity media such as sands and gravels, the volume of water released to the well from storage in the formation during early time pumpage is usually significantly larger than the volume of water stored in the well and thus little error is introduced. Conversely, in low-storativity media such as fractured rock, the volume of water released from storage in the well is often substantially larger than the volume of water released from the formation due to storage during pumping. If the Theis curve is used to analyse pumping test data obtained from a low-storativity environment, transmissivity will be significantly underestimated and storativity overestimated [*Prats and Scott*, 1976]. The obvious remedy to this problem is to diminish the well bore storage capacity of the pumping well. This can be achieved for tests conducted in fractured rock, by packing-in the well (isolating the test zone with packers or bridge plugs), although this is often impractical due to the size of downhole pumps. In the case where the well bore storage capacity of the well can not be reduced, an alternate analytical method is required with which to analyze drawdown data.

Pumping tests conducted in low-storativity media are also commonly influenced by a zone of permeability reduction or enhancement adjacent to the well [*Earlougher*, 1977]. This zone is known as the skin region and depending on the thickness and permeability contrast between the skin region and the formation can significantly affect the observation well response. Skin regions usually develop during the drilling of wells as a consequence of drilling mud or rock flour invasion. Consequently, most skin regions are of lower permeability than the formation. Under some circumstances, depending on the drilling method and the formation, substantial spalling and fracturing of the borehole wall may act to increase the permeability in the region adjacent to the well. Geochemical precipitation or dissolution after drilling may also reduce or enhance permeability. In any case, the thickness of the skin region can range from a few millimeters to several meters and thus must be considered, in the analysis of pumping tests, as a separate zone of radial flow contiguous with radial flow in the formation.

The effect of both well bore storage and the skin region on the results of pumping tests has long been recognized in the petroleum industry [*van Everdingen and Hurst*, 1949; *Hawkins*, 1956] and more recently by groundwater scientists [*Papadopolus and Cooper*, 1967; *Moench*, 1985]. Most of the research on this topic has been conducted by the petroleum industry and there are solutions available which account for well bore storage and infinitesimally thin skin in the pumping well [*Sandal et al.*, 1976; *Chu et al.*, 1980] and both the pumping well and observation wells [*Tongpenyai*

Paper number 89WR01011.
0043-1397/89/89WR-01011$05.00

and Raghaven, 1981; *Obge*, 1984; *Ogbe and Brigham*, 1984]. The mathematical treatment used in these models to account for the skin region, however, is only an approximation and the hydraulic head drop across the skin is presumed to occur under steady flow conditions. Mathematically, this leads to an inner boundary condition which provides continuity between the head in the well (h_w) and head in the formation (h):

$$h_w = h|_{r=r_w} - \Delta h_K \tag{1}$$

where Δh_K is the head drop across the skin. According to (1), the skin region must be of zero thickness and storativity. Because, in nature, the skin region is usually of finite thickness, a new model is required in which the medium is represented by two regions of radial flow each with individual transmissivity, storativity, and thickness. Composite models of this type have been developed for pumping test problems [*Karasaki*, 1986; *Butler*, 1988] but none are available in which well bore storage is considered.

The purpose of this paper is to present an analytical model for a pumping test which accounts for a composite medium of a skin region and formation region including well bore storage at the pumping well. In addition, a comparison to the case for infinitesimally thin skin (equation (1)) will be made and the influence of well bore storage on disguising the thickness and hydraulic properties of the skin will be investigated. Using the solution for the skin region, the influence of outer boundary conditions on pumping test results will also be studied.

Mathematical Development of the Composite Model

The following mathematical development is similar to that for other composite models of this type [*Wang et al.*, 1978; *Moench and Hsieh*, 1985; *Karasaki*, 1986; *Butler*, 1988] with the exception of the well bore storage condition expressed in equation (6). The basic assumptions that apply to most pumping test models can also be applied here: (1) the fluid is slightly compressible and of constant viscosity, (2) the medium is homogeneous and isotropic, and (3) the pumping well and observation well penetrate the entire thickness of the formation. A governing equation is required for each region of radial flow. The equations for the skin region and the formation are given in dimensional format as

$$\frac{\partial^2 s_1}{\partial r^2} + \frac{1}{r}\frac{\partial s_1}{\partial r} = \frac{S_1}{T_1}\frac{\partial s_1}{\partial t} \qquad r_w \le r \le r_s \tag{2}$$

$$\frac{\partial^2 s_2}{\partial r^2} + \frac{1}{r}\frac{\partial s_2}{\partial r} = \frac{S_2}{T_2}\frac{\partial s_2}{\partial t} \qquad r \ge r_s \tag{3}$$

respectively, where subscripts 1 and 2 denote the skin and formation regions, s is drawdown, T and S are transmissivity and storativity, respectively, r is radial distance, r_w is the pumping well radius, r_s is the radius of the skin region, and t is time. The initial conditions for (2) and (3) are

$$s_1(r, 0) = s_2(r, 0) = 0 \qquad r_w < r < \infty \tag{4}$$

The outer boundary condition for (3) is

$$s_2(\infty, t) = 0 \tag{5}$$

and the inner boundary condition which describes well bore storage is given as

$$2\pi r_w T_1 \, \partial s_1/\partial r|_{r=r_w} = C \, ds_w/dt - Q \tag{6}$$

where s_w is the drawdown in the well, Q is flow rate, and C is a constant describing well bore storage capacity, equal to πr_c^2 for open pumping wells (r_c is the radius of the standpipe which may be smaller or larger than the radius of the well). The initial condition for (6) is

$$s_w(0) = 0 \tag{7}$$

Continuity between the well and the skin region is given by

$$s_w(r_w, t) = s_1(r_w, t) \tag{8}$$

and continuity between the skin region and the formation is given by

$$s_1(r_s, t) = s_2(r_s, t) \tag{9}$$

$$T_1 \frac{\partial s_1(r_s, t)}{\partial r} = T_2 \frac{\partial s_2(r_s, t)}{\partial r} \tag{10}$$

A solution to (2) and (3) with respect to (4)–(10) can be found in a straightforward manner using the Laplace transform method. Details of the solution method are given in the appendix. The solution is obtained using dimensionless groupings similar to those given by *Moench and Hsieh* [1985]:

$$t_D = T_2 t/S_2 r_w^2 \qquad C_D = C/2\pi r_w^2 S_2 \tag{11a}$$

$$r_D = r/r_w \qquad r_{DS} = r_s/r_w \tag{11b}$$

$$\Phi_{D1} = \frac{2\pi T_2 s_1}{Q} \qquad \Phi_{D2} = \frac{2\pi T_2 s_2}{Q} \qquad \Phi_{WD} = \frac{2\pi T_2 s_w}{Q} \tag{11c}$$

$$\alpha = T_2/T_1 \qquad \gamma = S_1/S_2 \tag{11d}$$

where t_D is dimensionless time, C_D is the dimensionless well bore storage coefficient, and Φ_D is dimensionless drawdown.

The solutions in the Laplace domain for Φ_{D1}, Φ_{D2}, and Φ_{WD} are given as

$$\bar{\Phi}_{D1} = \frac{\alpha}{p}\frac{[\psi_2 K_0((p\alpha\gamma)^{1/2} r_D) - \psi_1 I_0((p\alpha\gamma)^{1/2} r_D)]}{(\psi_2\xi_2 - \psi_1\xi_1)} \tag{12}$$

$$\bar{\Phi}_{D2} = \frac{\alpha}{p^{3/2} r_{DS}}\frac{K_0(\sqrt{p}\, r_D)}{(\psi_2\xi_2 - \psi_1\xi_1)} \tag{13}$$

$$\bar{\Phi}_{WD} = \frac{\alpha}{p}\frac{[\psi_2 K_0((p\alpha\gamma)^{1/2}) - \psi_1 I_0((p\alpha\gamma)^{1/2})]}{(\psi_2\xi_2 - \psi_1\xi_1)} \tag{14}$$

respectively, where the overbar denotes the Laplace transformed parameter, p is the Laplace variable, and

$$\xi_1 = \alpha C_D p I_0((p\alpha\gamma)^{1/2}) - (p\alpha\gamma)^{1/2} I_1((p\alpha\gamma)^{1/2}) \tag{15}$$

$$\xi_2 = \alpha C_D p K_0((p\alpha\gamma)^{1/2}) + (p\alpha\gamma)^{1/2} K_1((p\alpha\gamma)^{1/2})$$

$$\psi_1 = \alpha K_0((p\alpha\gamma)^{1/2} r_{DS}) K_1(\sqrt{p}\, r_{DS}) - (\alpha\gamma)^{1/2} K_0(\sqrt{p}\, r_{DS}) K_1((p\alpha\gamma)^{1/2} r_{DS}) \tag{16}$$

$$\psi_2 = \alpha I_0((p\alpha\gamma)^{1/2} r_{DS}) K_1(\sqrt{p}\, r_{DS}) + (\alpha\gamma)^{1/2} I_1((p\alpha\gamma)^{1/2} r_{DS}) K_0(\sqrt{p}\, r_{DS})$$

where K_0, K_1, I_0, and I_1 are modified Bessel functions.

Analytical inversion of (12)–(14) is probably possible using

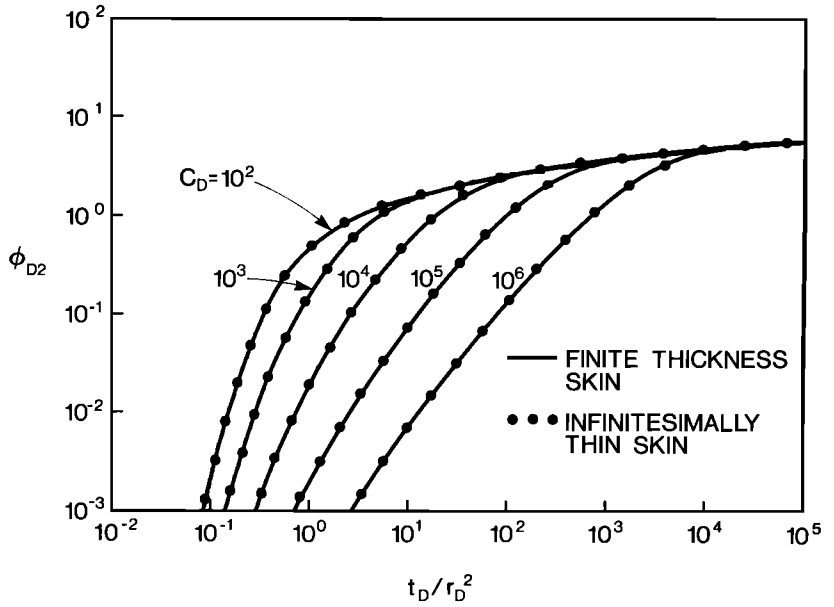

Fig. 1. Comparison of the pumping test model accounting for well bore storage and infinitesimally thin skin to the model developed herein. Comparison is made for the case where r_{DS} equals 1.1 and α equals 100 (S_K of 9.5) for C_D from 10^2 to 10^6 (C_D of 10^6 is the rightmost curve) and r_D equals 100.

contour integration (see *Karasaki et al.* [1985] for an example); however, this will lead to an infinite integral containing several Bessel functions that will be very computationally inefficient to numerically evaluate. Therefore for the following discussion, the solutions are numerically inverted using the *Talbot* [1979] algorithm. The accuracy of the Talbot algorithm has been established using other, similar well test problems [*Novakowski*, 1989] and was found to be accurate within at least three significant figures in comparison to analytical inversions.

Verification of the Solution

Verification of the solutions (12)–(14) is performed by comparison to existing solutions for similar well testing problems with slightly different boundary conditions. The solution in Laplace space for dimensionless drawdown in a uniform medium including well bore storage effects is given as [*Papadopolus and Cooper*, 1967]

$$\bar{\Phi}_D = \frac{K_0(\sqrt{p}\, r_D)}{p[C_D p K_0(\sqrt{p}) + \sqrt{p} K_1(\sqrt{p})]} \tag{17}$$

Equation (17) can also be found from (13) by setting α and γ equal to one for a uniform medium. In addition, by negating well bore storage, the solution accounting for a composite medium with no well bore storage can be found. Again, using (13), this is given as

$$\Phi_{D2} = \frac{\alpha}{p^{3/2} r_{DS}} \frac{K_0(\sqrt{p}\, r_D)}{[(p\alpha\gamma)^{1/2} K_1((p\alpha\gamma)^{1/2})\psi_2 + (p\alpha\gamma)^{1/2} I_1((p\alpha\gamma)^{1/2})\psi_1]} \tag{18}$$

Equation (18) is algebraically similar to the solution obtained for this problem by *Karasaki* [1986] and when numerically inverted for several test cases, (18) overlies Karasaki's solution. Comparison to the solution accounting for well bore storage and infinitesimally thin skin is also possible using approximations for the modified Bessel functions as the arguments approach zero (i.e., $\alpha \to 0$). This approach was employed by *Moench and Hsieh* [1985] and they discovered that using a skin factor S_K equal to

$$S_K = \alpha \ln (r_{DS}) \tag{19}$$

infinitesimally thin skin can be made equivalent to the composite case. Therefore using (19), (13) can be reduced to

$$\bar{\Phi}_D = \frac{K_0(\sqrt{p}\, r_D)}{p\{\sqrt{p}\, K_1(\sqrt{p}) + C_D p[K_0(\sqrt{p}) + S_K \sqrt{p} K_1(\sqrt{p})]\}} \tag{20}$$

which is the solution as obtained by *Sandal et al.* [1978] accounting for well bore storage and infinitesimally thin skin. A comparison was made between (13) and (20) at an α of 100, an r_D of 100, and a small r_{DS} of 1.1, where S_K in (20) was calculated using (19). Type curves ranging over five orders of magnitude of C_D were numerically generated for the comparison (Figure 1). No identifiable difference is discernable in the plotted curves. As suggested by *Moench and Hsieh* [1985], this comparison may not hold as r_{DS} increases. This will be investigated in the following section.

Discussion

In the following discussion, γ is fixed at one for all example type curves. This is justified based on the assumption that the development of the skin region is solely a result of a difference in permeability to that of the formation and that no contrasts in formation compressibility or fracture stiffness occur concomitantly.

Due to the large number of variables, use of the solutions (12)–(14) to uniquely interpret field data obtained from

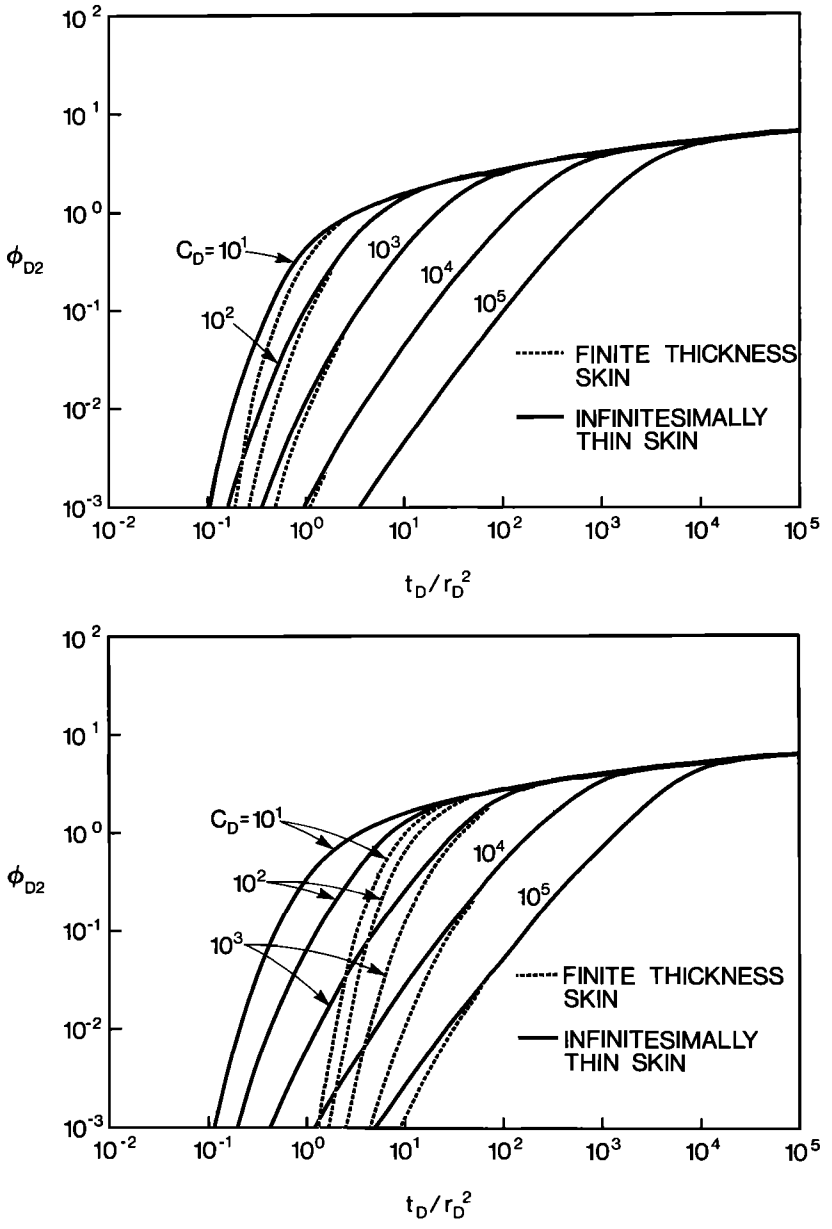

Fig. 2. Comparison of the infinitesimally thin skin solution to the finite thickness skin solution at an r_D of 100, α of 100, C_D of 10^1 to 10^5, and an r_{DS} of (top) 10 and (bottom) 50.

pumping tests may prove difficult and thus a field example is not given herein. However, the influence of some of the parameters on expected field results, particularly C_D, r_{DS}, and α, can be investigated by generating example type curves for various values and drawing comparison on the basis of the shape of the type curves and position in dimensionless time. Example type curves are employed rather than sensitivity coefficients, so that the effects of the individual combinations of parameters are visualized in a manner similar to that in which field data is presented.

Comparison to Infinitesimally Thin Skin

As we have already seen, there may be some conditions in which the solution accounting for infinitesimally thin skin and well bore storage may adequately substitute for the solution developed herein. To investigate the influence of the skin thickness, type curves were generated with α equal to 100 at an r_D of 100 for four successively larger r_{DS} starting at 1.1 ranging to 50. This configuration corresponds to a field condition in which an observation well is located about 10 m away from a 0.1-m-radius pumping well. A skin region which has a permeability two orders of magnitude less than the formation is present at the pumping well and ranges in thickness from 0.11 to 5.0 m. Figure 2 shows the case for r_{DS} equal to 10 and 50 against the equivalent curves generated using (19) and (20). As is evident, the effects of increasing skin thickness act to delay the early time drawdown at the observation well for smaller values of C_D. This is most pronounced at the largest skin thickness of 5 m and the thin skin solution very poorly approximates these conditions here. At larger values of C_D (greater than 10^4), however, the thin skin approximates the composite model accurately.

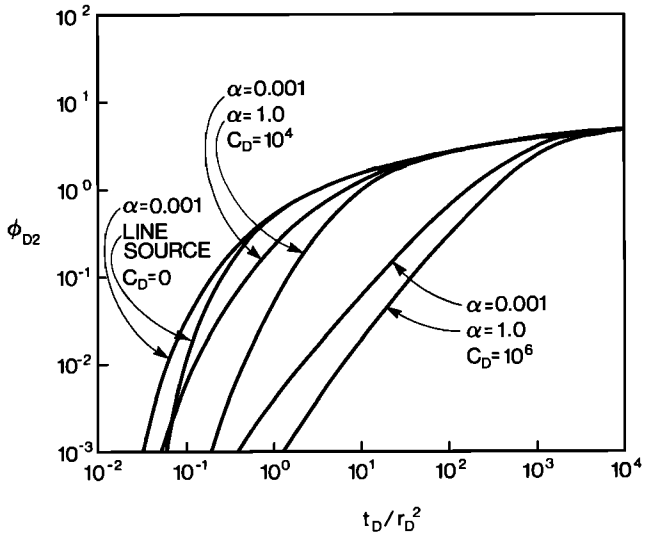

Fig. 3. Type curves for α of 10^0 and 10^{-3} at r_D equal to 100, r_{DS} equal to 50, and C_D of 0, 10^4, and 10^6.

Therefore to identify finite skin regions of low permeability in pumping test data, the tests should be conducted with expected well bore storage coefficients of less than 10^5. Otherwise, well bore storage will entirely mask the skin effect.

Effect of Higher Permeability in the Skin Region

Higher permeability in the skin region relative to that in the formation, also known as negative skin [*Jargon*, 1976; *Sandal et al.*, 1978], is difficult to simulate using an infinitesimally thin skin [*Sandal et al.*, 1978]. This is especially true when using Laplace transform techniques with $C_D > 0$. *Agarwal et al.* [1970] suggested an approximation for this case in which the skin factor is set to zero in the solution and the well radius is then adjusted according to the actual negative skin factor desired, using $r_w' = r_w \exp(-S_K)$. This approximation appears to work well for simulating drawdown in the pumped well [*Agarwal et al.*, 1970; *Ramey and Agarwal*, 1972] but has never been successfully used for drawdown at the observation well. Therefore the composite model presented here provides the only valid means of simulating negative skin without employing a numerical method.

Figure 3 shows three sets of type curves for an α of 10^{-3} and 1 for each set, at a C_D of 10^6, 10^4, and 0, an r_D of 100, and an r_{DS} of 50. In this case, the influence of well bore storage is to enhance the effect of negative skin. For example, at C_D equal to zero the difference between α equal to 1 and α equal to 10^{-3} is marginally apparent only at early time. During pumping tests, good quality, early time data is rarely obtained unless electronic recording devices are used, and therefore a negative skin might never be detected. Conversely, at larger C_D the negative skin acts to advance the rate of drawdown at a different slope than the case for α equal to 1 and the difference between the two curves can be clearly identified until the asymptote is reached. This is different than the case for positive skin at large C_D in which the curves are simply shifted to the left toward the time origin without change in slope. Therefore if a negative skin is suspected to be present, pumping tests should be conducted in the field setting with well bore storage greater than zero.

Figure 4 shows a range of type curves for α from 10^{-4} to 10^4 at a C_D of 10^4, r_D of 100, and r_{DS} of 50. The effect of the contrast in permeability between the skin region and the formation appears to be considerably less for negative skin than for positive skin in this case. The type curve for α equal to 10^4 is shifted to the left by several orders of magnitude in t_D/r_D^2, while for α equal to 10^{-4} the curve is shifted to the right by only one order of magnitude. This is exemplified as C_D is diminished toward zero. The slope of the early time part of the curve for positive skin remains about the same, irrespective of the magnitude of α. In addition, as shown in Figure 5, for C_D equal to 10^5 and 0, the position of the type curve is relatively insensitive to the skin thickness for negative skin. Consequently, determining the properties of

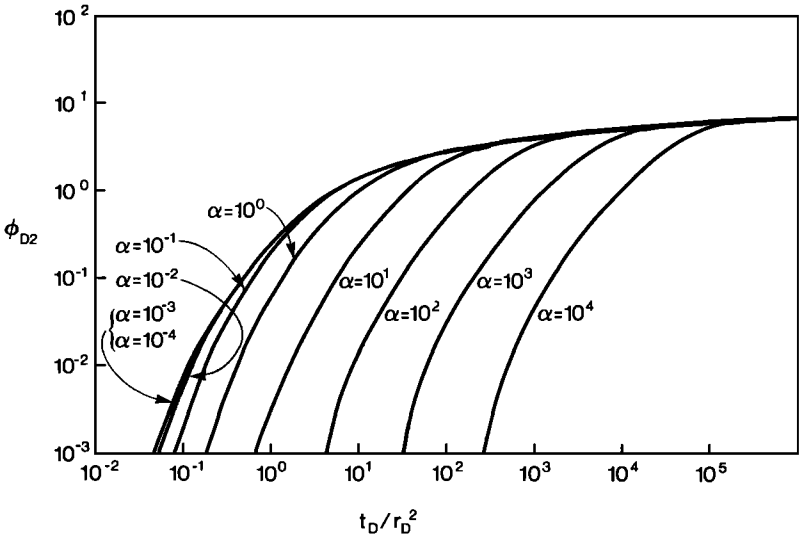

Fig. 4. Type curves for the case when r_D equals 100, r_{DS} equals 50, C_D equals 10^4, and α ranges from 10^{-4} to 10^4.

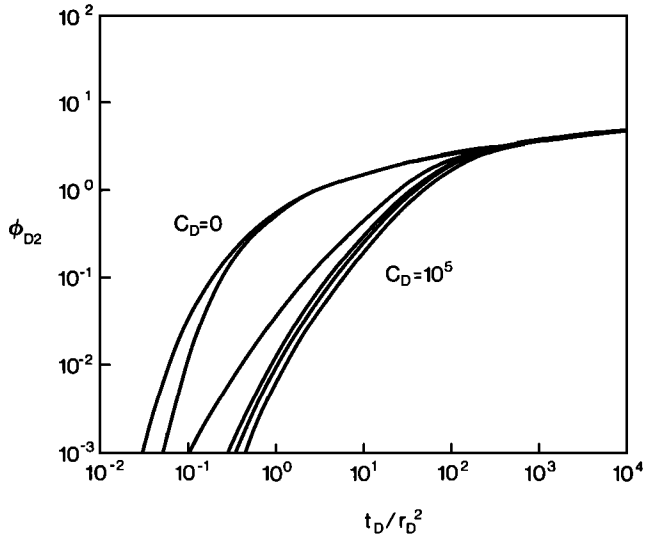

Fig. 5. Two families of type curves at C_D of 0 and 10^5 for r_D equal to 100, α equal to 10^{-3}, and r_{DS} of 1.1, 5.0, 10.0, and 50.0, where r_{DS} of 50 is the leftmost curve in each family.

finite thickness skin is much more difficult for negative skin than for positive skin.

Effect of Radial Distance

The type curves generated for Figures 1 through 5 are for an r_D of 100. In many field settings r_D will likely exceed 100 ranging up to 1000 or greater. As is apparent in Figures 1–5, all type curves trend asymptotically toward the Theis line source solution at large t_D/r_D^2. Intuitively, therefore the behavior of the composite model observed at early time should be diminished at larger r_D. For example, the effect of a positive finite thickness skin (α = 1000) with a thickness of r_{DS} equal to 50 diminishes with r_D increasing from 100 to 2000, as shown in Figure 6. At the largest r_D the type curve for C_D equals 0, differs only slightly from the line source solution for a uniform medium and only at small t_D/r_D^2. However, the steep slope characteristic of finite thickness skin at low C_D is still clearly identifiable at r_D of 500. Positive skin effects should be easily identified at smaller C_D for r_D anywhere between 100 and less than 1000. Again, although well bore storage effects are also diminished by increasing radial distance, the presence of $C_D > 0$ acts to mask the influence of finite thickness skin. Negative skin is similarly influenced by increasing radial distance.

Influence of Outer Boundaries

Pumping tests conducted in low-storativity formations such as fractured rock are often observed to be influenced by far-field or outer boundary conditions [*Raven*, 1986]. Such conditions can manifest in the field setting as linear features such as faults and facies changes or as radial boundaries due to permeability reduction (finite fracture extent) or enhancement as a result of stress heterogeniety. The effect of linear features on pumping test results can not be investigated using the composite model developed here; however, radial boundaries can be investigated by expanding the skin region to the radial boundary and solving for drawdown in the skin region using (12).

Figure 7 shows dimensionless drawdown at α equal to 10, 1, and 0.2 for r_{DS} of 200 and 10^5 at r_D of 100 and 5000, respectively, and C_D equal to 10^3. Comparing the type curves for r_D of 100 and r_D of 5000, there is remarkably little difference in both the shape of the curves and position in t_D/r_D^2. Therefore even subtle changes in far-field permeability can be detected at large radial distance. In addition, permeability enhanced boundaries ($\alpha > 1$) strongly influence early to midtime data with the early time drawdown being characteristic of the steep slopes observed with positive

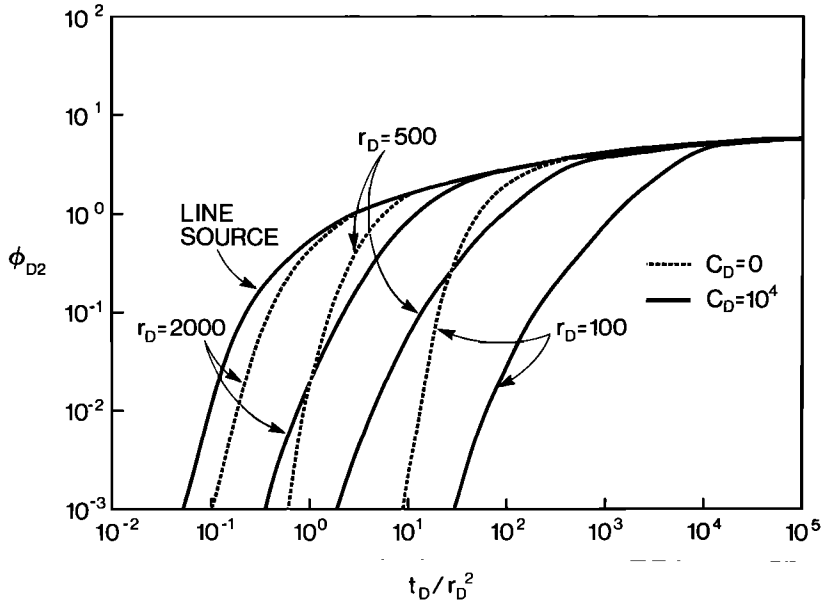

Fig. 6. Type curves for r_{DS} of 50, α of 10^3, and C_D of 0 and 10^4 for r_D of 100, 500, and 2000, as compared to the line source solution.

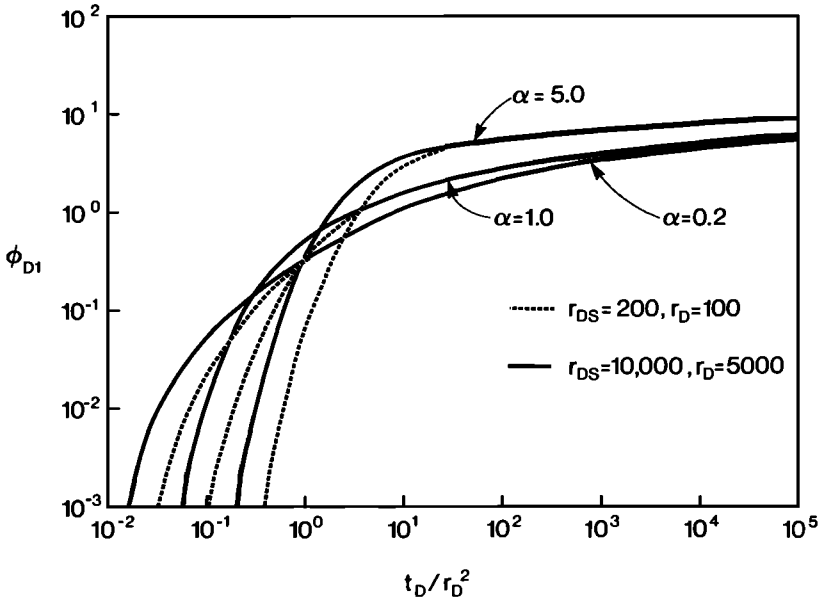

Fig. 7. Three pairs of type curves for α of 0.2, 1.0, and 5.0 with C_D equal to 10^3.

finite thickness skin (i.e., Figure 2). Permeability enhanced boundaries, however, can be distinguished from finite thickness skin at later time where drawdown follows the line source asymptote for the skin case and does not for the radial boundary case.

The influence of outer boundaries is illustrated in Figure 8 for a variety of α ranging from 0.001 to 1000 at an r_{DS} of 200 and an r_D of 100. Clearly, at α of 1000 the type curve is substantially different than the line source solution and such a field condition would be easily identifiable. However, at larger r_D, the actual onset of drawdown is dramatically delayed in t_D/r_D^2 such that observation may be abandoned during a field pumping test before initial drawdown is observed.

A more typical field condition is the case for a radial boundary of reduced permeability ($\alpha < 1$) which could result, for example, from a hydraulically propogated fracture of large extent. In this case, early time drawdown is advanced in t_D/r_D^2 and the slope of the early time data is diminished such that the change in drawdown is spread over

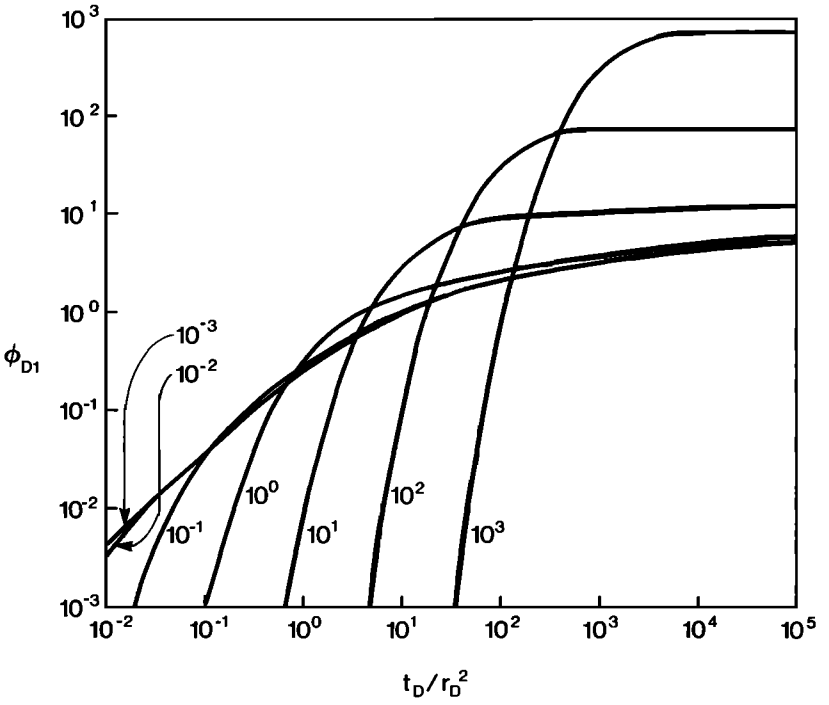

Fig. 8. Type curves for a range of α from 10^{-3} to 10^3 at C_D of 10^3, r_D of 100, and r_{DS} of 200.

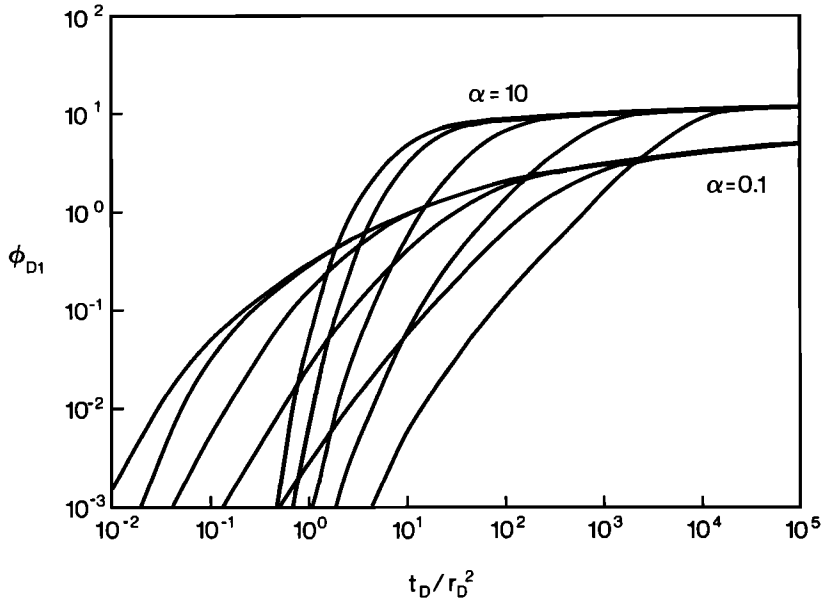

Fig. 9. Two families of type curves for α of 0.1 and 10. Each family is generated for the case where r_D equals 100, r_{DS} equals 200, and C_D ranges from 10^2 to 10^6.

several orders of magnitude of t_D/r_D^2 before the asymptote is reached. The magnitude of α has considerably less influence on the nature of the early time data relative to the permeability enhanced case and for small r_D, the actual early time shape may not be observed during field pumping tests. At larger r_D, the early time slope would be characteristic of a permeability reduced boundary (the shape of these curves at early time are unique). Late time data, although also characteristic and relatively independent of r_D, is asymptotic for most α (Figure 8). This means that without early time data, the nature of the reduced permeability boundary can not be characterized other than to identify that it exists.

The influence of well bore storage on detecting boundaries of reduced or enhanced permeability is shown in Figure 9 for C_D ranging from 10^2 to 10^6, α of 10 and 0.1 at r_{DS} of 200, and r_D of 100. Again, the shape of the curves for $\alpha > 1$ are similar to those for finite thickness skin (Figure 2) except that the late time asymptote has less slope than the line source solution. For $\alpha < 1$, well bore storage acts to delay the interception of the individual curves with the asymptote; i.e., the early time slope is extended in t_D/r_D^2. Therefore well bore storage effects do not mask the presence of boundaries of reduced permeability, however, due to the slope of the type curves, long-term data from pumping tests will be required for a suitable curve-matching procedure.

CONCLUSIONS

A composite analytical model was derived which accounts for well bore storage and a region of finite thickness skin present at a pumping well. Solutions in the Laplace domain were given for dimensionless drawdown in the borehole, skin region, and formation. On the basis of example type curves for which the contrast between permeability in the skin region versus that for the formation, the thickness of the skin region and the radial distance to the observation well were systematically varied, several observations can be made.

1. The approximation for infinitesimally thin skin can be used to analyze pumping test results where the skin thickness is very small relative to the radial distance to the observation well, i.e., $r_{DS}/r_D < 0.05$ approximately.

2. Where the positive skin region (permeability of the skin region less than the formation) is larger, the testing apparatus must be designed such that well bore storage effects are diminished. Accurate early time data will be needed to detect and characterize the contrast in permeability and skin region thickness.

3. Negative skin effects (permeability of the skin region greater than the permeability of the formation) are most easily identified at early to midtime using an apparatus having a large well bore storage.

4. Positive skin is more readily characterized than negative skin, although the presence of negative skin is more easily identifiable.

5. The influence of finite thickness skin can be identified in a fairly broad range of radial distance from the pumping well, i.e., r_D of 100–1000. Uniqueness is possible using the parameters α and r_{DS}.

6. The influence of the contrast in skin region versus formation permeability is much more pronounced for positive skin than for negative skin. The effect of the contrast for positive skin is to substantially delay initial drawdown at the observation well.

7. Early time drawdown is required to detect permeability reduced boundaries at large radial distances. At late time, the distance to a boundary or a zone of contrasting permeability cannot be distinguished.

8. Radial distance has little influence on diminishing the effect of far-field boundary conditions. Even subtle contrasts in permeability can be observed.

9. Well bore storage hides the early time influence of permeability reduced boundaries but not at late time. However, well bore storage effects also make it difficult to identify permeability enhanced boundaries at late time.

APPENDIX: SOLUTION METHOD

The solution of (2) and (3) is found using the Laplace transform method.The governing equation and associated boundary conditions are first made dimensionless using the groupings given in (11). The governing equations in dimensionless format are

$$\frac{\partial^2\Phi_{D1}}{\partial r_D^2}+\frac{1}{r_D}\frac{\partial\Phi_{D1}}{\partial r_D}=\alpha\gamma\frac{\partial\Phi_{D1}}{\partial t_D} \tag{A1}$$

$$\frac{\partial^2\Phi_{D2}}{\partial r_D^2}+\frac{1}{r_D}\frac{\partial\Phi_{D2}}{\partial r_D}=\frac{\partial\Phi_{D2}}{\partial t_D} \tag{A2}$$

the inner and outer boundary conditions are given by

$$\left.\frac{\partial\Phi_{D1}}{\partial r_D}\right|_{r_D=1}=\alpha C_D\frac{d\Phi_{WD}}{dt_D}-\alpha \tag{A3}$$

$$\Phi_{D1}(r_{DS}, t_D)=\Phi_{D2}(r_{DS}, t_D) \tag{A4}$$

$$\frac{\partial\Phi_{D1}(r_{DS}, t_D)}{\partial r_D}=\alpha\frac{\partial\Phi_{D2}(r_{DS}, t_D)}{\partial r_D} \tag{A5}$$

$$\Phi_{D1}(1, t_D)=\Phi_{WD}(1, t_D) \tag{A6}$$

$$\Phi_{D2}(\infty, t_D)=0 \tag{A7}$$

and the initial conditions for (A1), (A2), and (A3) are described by

$$\Phi_{D1}(r_D, 0)=\Phi_{D2}(r_D, 0)=0 \tag{A8}$$

$$\Phi_{WD}(0)=0 \tag{A9}$$

Application of the Laplace transform to (A1) and (A2) leads to the following subsidiary equations:

$$\frac{d^2\bar{\Phi}_{D1}}{dr_D^2}+\frac{1}{r_D}\frac{d\bar{\Phi}_{D1}}{dr_D}=\alpha\gamma p\bar{\Phi}_{D1} \tag{A10}$$

$$\frac{d^2\bar{\Phi}_{D2}}{dr_D^2}+\frac{1}{r_D}\frac{d\bar{\Phi}_{D2}}{dr_D}=p\bar{\Phi}_{D2} \tag{A11}$$

where the overbar denotes the Laplace transformed parameter, and p is the Laplace variable. Application of the Laplace transform to the boundary conditions (A3)–(A7) gives

$$d\bar{\Phi}_{D1}/dr_D|_{r_D=1}=\alpha C_D p\bar{\Phi}_{WD}-\alpha/p \tag{A12}$$

$$\bar{\Phi}_{D1}(r_{DS}, p)=\bar{\Phi}_{D2}(r_{DS}, p) \tag{A13}$$

$$\frac{d\bar{\Phi}_{D1}(r_{DS}, p)}{dr_D}=\alpha\frac{d\bar{\Phi}_{D2}(r_{DS}, p)}{dr_D} \tag{A14}$$

$$\bar{\Phi}_{D1}(1, p)=\bar{\Phi}_{WD}(1, p) \tag{A15}$$

$$\bar{\Phi}_{D2}(\infty, p)=0 \tag{A16}$$

The general solution of the ODE (A10) and (A11) are given by

$$\bar{\Phi}_{D1}=AI_0((p\alpha\gamma)^{1/2}r_D)+BK_0((p\alpha\gamma)^{1/2}r_D) \tag{A17}$$

$$\bar{\Phi}_{D2}=CI_0(\sqrt{p}r_D)+DK_0(\sqrt{p}\,r_D) \tag{A18}$$

and using (A16) to bound the solution, (A18) reduces to

$$\bar{\Phi}_{D2}=DK_0(\sqrt{p}\,r_D) \tag{A19}$$

To find the constants A, B, and D, the boundary conditions (A12), (A13), and (A14) are employed:

$$A(p\alpha\gamma)^{1/2}I_1((p\alpha\gamma)^{1/2})-B(p\alpha\gamma)^{1/2}K_1((p\alpha\gamma)^{1/2}))$$
$$=\alpha C_D p\bar{\Phi}_{WD}-\alpha/p \tag{A20}$$

$$AI_0((p\alpha\gamma)^{1/2}r_{DS})+BK_0((p\alpha\gamma)^{1/2}r_{DS})=DK_0(\sqrt{p}\,r_{DS}) \tag{A21}$$

$$A(p\alpha\gamma)^{1/2}I_1((p\alpha\gamma)^{1/2}r_{DS})-B(p\alpha\gamma)^{1/2}K_1((p\alpha\gamma)^{1/2}r_{DS})$$
$$=-D\alpha\sqrt{p}\,K_1(\sqrt{p}\,r_{DS}) \tag{A22}$$

and (A15) is used to remove $\bar{\Phi}_{WD}$ from (A20) to obtain

$$-A[\alpha C_D pI_0((p\alpha\gamma)^{1/2})-(p\alpha\gamma)^{1/2}I_1((p\alpha\gamma)^{1/2})]$$
$$-B[\alpha C_D pK_0((p\alpha\gamma)^{1/2})+(p\alpha\gamma)^{1/2}K_1((p\alpha\gamma)^{1/2})]=-\alpha/p \tag{A23}$$

Equations (A23), (A21), and (A22) can be solved using Cramer's rule to determine the constants A, B, and D, which are then substituted into (A17) and (A19) to obtain the solutions for $\bar{\Phi}_{D2}$ and $\bar{\Phi}_{D1}$. The solution for $\bar{\Phi}_{D2}$ is reduced to the form given by (13) using the identity [*Karasaki*, 1986]

$$I_0((p\alpha\gamma)^{1/2}r_{DS})K_1((p\alpha\gamma)^{1/2}r_{DS})$$
$$+I_1((p\alpha\gamma)^{1/2}r_{DS})K_0((p\alpha\gamma)^{1/2}r_{DS})=\frac{1}{(p\alpha\gamma)^{1/2}r_{DS}} \tag{A24}$$

The solution for drawdown in the pumping well, $\bar{\Phi}_{WD}$, is obtained using (A15).

NOTATION

- C well bore storage capacity, L^2.
- C_D dimensionless well bore storage coefficient, $C/2\pi r_w^2 S_2$.
- p Laplace variable.
- Q volumetric pumping rate, L^3/T.
- r radial distance, L.
- r_c radius of the standpipe, L.
- r_D dimensionless radial distance, r/r_w.
- r_{DS} dimensionless radius of the skin, r_s/r_w.
- r_s radius of the skin, L.
- r_w radius of the pumping well, L.
- r_w' effective pumping well radius, L.
- s drawdown, L.
- s_w drawdown in the pumping well, L.
- S storativity, dimensionless.
- S_K skin factor, dimensionless.
- t time, T.
- t_D dimensionless time, $T_2 t/S_2 r_w^2$.
- T transmissivity, L^2/T.
- α ratio of the permeability of the formation over the skin permeability, T_2/T_1.
- γ ratio of the storativity of the skin over the formation storativity, S_1/S_2.

Subscripts 1 and 2 denote skin region and formation, respectively; I_0, I_1, K_0, and K_1 are modified Bessel functions.

Acknowledgments. The author would like to extend gratitude to E. Sudicky for several helpful suggestions proffered during the course of this study, and for reviewing the draft manuscript. O.

Resler assisted with the numerous computer runs required for the generation of the example type curves.

REFERENCES

Agarwal, R. G., R. Al-Hussainy, and H. J. Ramey, Jr., An investigation of wellbore storage and skin effect in unsteady liquid flow, 1, Analytical treatmet, *Soc. Pet. Eng. J.*, *10*(3), 279–290, 1970.

Butler, J. J., Jr., Pumping tests in nonuniform aquifers—The radially symmetric case, *J. Hydrol.*, *101*, 15–30, 1988.

Chu, W. C., J. Garcia-Rivera, and R. Raghaven, Analysis of interference test data influenced by wellbore storage and skin at the flowing well, *J. Pet. Technol.*, *32*, 263–269, 1980.

Earlougher, R. C., Jr., Advances in well test analysis, *Soc. Pet. Eng. of AIME Special Monograph*, vol. 5, Society of Petroleum Engineers, Richardson, Tex., 1977.

Hawkins, M. F., Jr., A note on the skin effect, *Trans. Am. Inst. Min. Metall. Pet. Eng.*, *207*, 356–367, 1956.

Jargon, J. R., Effect of wellbore storage and well bore damage at the active well on interference test analysis, *J. Pet. Technol.*, *28*, 851–858, 1976.

Karasaki, K., Well test analysis in fractured media, Ph.D. thesis, 239 pp., Univ. of Calif., Berkeley, 1986.

Karasaki, K., P. A. Witherspoon, and J. C. S. Long, A new analytical model for fracture-dominated reservoirs, paper presented at Proc. 60th Ann. Tech. Conf., Soc. Pet. Eng., Las Vegas, Nev., September 1985.

Moench, A. F., Transient flow to a large-diameter well in an aquifer with storative semiconfining layers, *Water Resour. Res.*, *21*(8), 1121–1131, 1985.

Moench, A. F., and P. A. Hsieh, Analysis of slug test data in a well with finite thickness skin, paper presented at 17th International Congress, Int. Assoc. Hydrogeol., Tucson, Ariz., January 1985.

Novakowski, K. S., Analysis of aquifer tests in fractured rock: A review of the physical background and design of a computer program for generating type curves, *Groundwater*, in press, 1989.

Ogbe, D. O., Pulse testing in the presence of wellbore storage and skin effects, Ph.D. thesis, Stanford Univ., Stanford, Calif., 1984.

Ogbe, D. O., and W. E. Brigham, A model for interference testing with wellbore storage and skin effects at both wells, paper presented at 59th Annual Technical Conference, Soc. Pet. Eng., Houston, Tex., September 1984.

Papadopolus, I. S., and H. H. Cooper, Jr., Drawdown in a well of large diameter, *Water Resour. Res.*, *3*(1), 241—244, 1967.

Prats, M., and J. B. Scott, Effect of wellbore storage on pulse test pressure response, *J. Pet. Technol.*, *28*, 707–709, 1976.

Ramey, H. J., Jr., and R. G. Agarwal, Annulus unloading rates and well bore storage, *Soc. Pet. Eng. J.*, *24*, 453–462, 1972.

Raven, K. G., Hydraulic characterization of a small ground-water flow system in fractured monzonitic gneiss, *Pap. 30*, 133 pp., Nat. Hydrol. Res. Inst., Ottawa, Canada, 1986.

Sandal, H. M., R. N. Horne, H. J. Ramey, and J. W. Williamson, Interference testing with wellbore storage and skin effects at the produced well, paper presented at 53rd Annual Technical Conference, Soc. Pet. Eng., Houston, Tex., October 1978.

Talbot, A., The accurate numerical inversion of Lsaplace transforms, *J. Inst. Math. Applic.*, *23*, 97–120, 1979.

Tongpenyai, Y., and R. Raghaven, The effect of wellbore storage and skin on interference test data, *J. Pet. Technol.*, *33*, 151–160, 1981.

van Everdingen, A. F., and W. Hurst, The application of the Laplace transformation to flow problems in reservoirs, *Trans. Am. Inst. Min. Metall. Pet. Eng.*, *186*, 305–324, 1949.

Wang, J. S. Y., T. N. Narasimhan, C. F. Tsang, and P. A. Witherspoon, Transient flow in tight fractures, *Rep. LBL-7027*, pp. 103–116, Lawrence Berkeley Lab., Berkeley, Calif., 1978.

K. S. Novakowski, National Water Research Institute, 867 Lakeshore Road, P.O. Box 5050, Burlington, Ontario, Canada L7R 4A6.

(Received November 10, 1988;
revised May 11, 1989;
accepted May 16, 1989.)